Quantifying the role of climate and landscape characteristics on hydrologic partitioning and vegetation response

Hal Voepel,[1] Benjamin Ruddell,[2] Rina Schumer,[1] Peter A. Troch,[3] Paul D. Brooks,[3] Andrew Neal,[3] Matej Durcik,[3] and Murugesu Sivapalan[4]

Received 26 August 2010; revised 23 May 2011; accepted 10 June 2011; published 10 August 2011.

[1] There is no consensus on how changes in both temperature and precipitation will affect regional vegetation. We investigated controls on hydrologic partitioning at the catchment scale across many different ecoregions, and compared the resulting estimates of catchment wetting and vaporization (evapotranspiration) to remotely sensed indices of vegetation greenness. The fraction of catchment wetting vaporized by plants, known as the Horton index, is strongly related to the ratio of available energy to available water at the Earth's surface, the aridity index. Here we show that the Horton index is also a function of catchment mean slope and elevation, and is thus related to landscape characteristics that control how much and how long water is retained in a catchment. We compared the power of the components of the water and energy balance, as well as landscape characteristics, to predict Normalized Difference Vegetation Index (NDVI), a surrogate for vegetation productivity, at 312 Model Parameter Estimation Experiment (MOPEX) catchments across the United States. Statistical analysis revealed that the Horton index provides more precision in predicting maximum annual NDVI for all catchments than mean annual precipitation, potential evapotranspiration, or their ratio, the aridity index. Models of vegetation productivity should emphasize plant-available water, rather than just precipitation, by incorporating the interaction of climate and landscape. Major findings related to the Horton index are: (1) it is a catchment signature that is relatively constant from year-to-year; (2) it is related to specific landscape characteristics; (3) it can be used to create catchment typologies; and (4) it is related to overall catchment greenness.

Citation: Voepel, H., B. Ruddell, R. Schumer, P. A. Troch, P. D. Brooks, A. Neal, M. Durcik, and M. Sivapalan (2011), Quantifying the role of climate and landscape characteristics on hydrologic partitioning and vegetation response, *Water Resour. Res., 47*, W00J09, doi:10.1029/2010WR009944.

1. Introduction

[2] Terrestrial vegetation controls the fate of the majority of soil water through root uptake and transpiration, and is thus a first-order control on the water balance of watersheds [*Brutsaert*, 1988]. The amount of water vaporized (or transpired) by an ecosystem (V, Figure 1) is a complex function of species composition and density, plant biochemistry and physiology, nutrient availability, soil and landscape structure, atmospheric temperature, carbon dioxide concentration, and air humidity. However, the dominant factor in determining interbiome variability in use of available energy by vegetation to evaporate water is the variation in soil wetting due to precipitation [*L'vovich*, 1979; *Shuttleworth*, 1988]. Shifts in regional temperature and precipitation patterns caused by a combination of anthropogenic and cyclical climate changes complicate the prediction of the hydrologic response of terrestrial ecosystems [*Wagener*, 2007]. Current methods for the prediction of ecohydrological systems response to a changing climate is based on historical observations and assumptions of system stationarity, which does not provide a reliable guide for the future acclimation of vegetation or changes in watershed structure [*Milly et al.*, 2008].

[3] It is essential for hydrologists to improve the understanding of the controls on the growth and water use of terrestrial ecosystems in order to predict the effects of climate change and improve management of watersheds for flood control, water supply, biodiversity, and environmental watershed services. In addition, an accurate understanding of evapotranspiration remains a key limitation in the current representation of land/atmosphere moisture and energy feedbacks in regional and global climate modeling [*Hutjes et al.*, 1998]. Evapotranspiration is governed primarily by the availability of soil water, the net radiation balance at the land surface, and the atmosphere's ability to absorb evaporated moisture. These factors are controlled to first order by the mean annual state of the regional or biome-scale climate as described by Budyko's Aridity Index (A), which is the

[1]Division of Hydrologic Sciences, Desert Research Institute, Reno, Nevada, USA.
[2]Department of Engineering, Arizona State University—Polytechnic, Mesa, Arizona, USA.
[3]Department of Hydrology and Water Resources, University of Arizona, Tucson, Arizona, USA.
[4]Department of Civil and Environmental Engineering, University of Illinois at Urbana-Champaign, Urbana, Illinois, USA.

0043-1397/11/2010WR009944

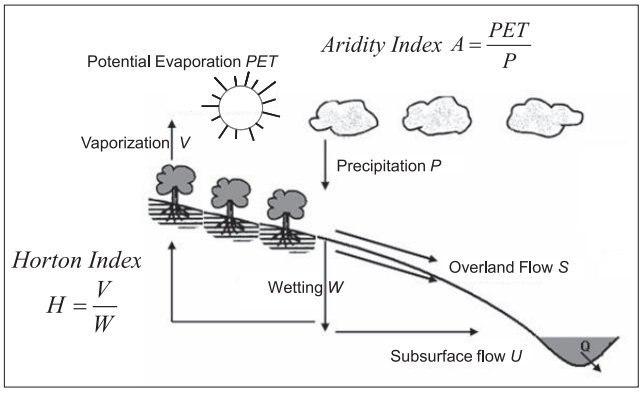

Figure 1. A conceptual model of hydrologic water balance partitioning at the land surface.

ratio of the annual mean potential evapotranspiration (PET, a function of air temperature, relative humidity, and net radiation at the land surface) to precipitation (P, Figure 1) [*Budyko*, 1974]. Recent work demonstrates that the timing, duration, and seasonality of rainfall events, as well as factors such as vegetation dynamics, soil moisture storage carryover, and topography, can become important controls on local scale or intrabiome V, especially in arid climates [*Donohue et al.*, 2007; *Gerrits et al.*, 2009; *Porporato et al.*, 2004; *Yang et al.*, 2009; *Zhang et al.*, 2008].

[4] While it is reasonable to suggest that rainfall timing, topography, vegetation dynamics, and moisture storage can be important controls on V, accurate quantification and modeling of these controls on V for the Earth's diverse terrestrial plant ecosystems remains a daunting challenge and an area of intense focus for contemporary ecohydrologists [*Thompson et al.*, 2011a, 2011b]. The identification of optimality principles and emergent patterns governing V [*Eagleson*, 1978; *Hatton et al.*, 1997; *Schymanski et al.*, 2007; *Schymanski*, 2008] is one promising approach to help constrain models of such a complex process. In one such pattern, the annual mean of the ratio of V to the plant-available water (W, Figure 1), known as the Horton index (H), approaches unity in more arid ecosystems, and in all ecosystems during the driest years [*Horton*, 1933; *Troch et al.*, 2009]. *Horton* [1933] hypothesized that H remains relatively constant (compared to the interannual variability of precipitation) within a watershed between years (with all watersheds converging toward H=1 in drier years) because plant ecosystems are adapted to maximize H given variability in the availability of water and energy. H is a function of the energy and water available to plants, including all landscape controls on the partitioning of precipitation into storm runoff (or quick flow or overland flow, S, Figure 1), subsurface flow (or slow flow or base flow, U, Figure 1), and plant-available water (or wetting, W, Figure 1). The Horton index of a watershed is therefore conceptually analogous to the aridity index, A, in that it is a function of climate-driven water and energy availability, except that plant available water in H is controlled by the topography and soils. The observations by *Horton* [1933] and *Troch et al.* [2009] are paralleled by the finding that all terrestrial vegetation biomes are adapted to converge to a common maximum rain-use efficiency (RUE), which is the ratio of annual mean net primary productivity (ANPP) to P in a biome [*Huxman et al.*, 2004].

[5] The Horton index thus represents a tool to guide the development of ecohydrologic theory at the catchment scale, to explore interactions between ecological and hydrologic processes, and the role of landscape properties and climate variability, including climate-landscape interaction, in the structure of catchment vegetation ecosystems and hydrologic partitioning [*Thompson et al.*, 2011b]. The Horton index is a dimensionless parameter related to the water balance theory suggested by *L'vovich* [1979] that explains the interannual variability of hydrologic partitioning, storage, and release. This index of hydrologic partitioning can be predicted empirically from Ponce and Shetty's functional model that builds upon this theory [*Ponce and Shetty*, 1995; *Sivapalan et al.*, 2011].

[6] Use of an independently derived measure of ecosystem response to variations in W and V would assist in the assessment of the usefulness of H to predict ecosystems response, and to compare with the use of A, P, and V to predict this response for a wide variety of watersheds [*Troch et al.*, 2009]. Remotely sensed measurements of the watershed's vegetation greenness (i.e., Normalized Difference Vegetation Index, NDVI) provide a logical choice, because satellite products are available for all watersheds, they are able to resolve spatial variability in vegetation, and greenness products are frequently used to model ecosystem productivity, evapotranspiration, and surface radiation balances [*Choudhury*, 1994; *Fisher et al.*, 2008; *Frouin and Pinker*, 1995; *Goetz and Prince*, 1999; *Hanan et al.*, 1995; *Szilagyi et al.*, 1998]. NDVI is sensitive to the hydrology of terrestrial ecosystems [*Brooks et al.*, 2011], and is therefore a useful independent measure on which to compare the accuracy of hydrological water balance models based on P, V, A, and H.

[7] The primary goal of this paper is to assess the role of climate and landscape characteristics on the water balance of catchment ecosystems across the conterminous USA. Our analysis considers watersheds as naturally defined ecosystems that integrate climate variability, vegetation processes, and physical landscape properties. Our specific research questions are (1) What catchment-scale landscape and regional-scale climate properties explain intercatchment Horton index variability?, and (2) Is the Horton index an efficient predictor of catchment-scale vegetation greenness (compared solely with climate information)?

[8] This paper is organized as follows: In section 2 we discuss the selection of Model Parameter Estimation Experiment (MOPEX) watersheds for our analysis, the derivation

of several physical landscape properties for these watersheds from existing data sources, the selection and preprocessing of streamflow, PET, and NDVI data products, the computation of H and other indices, and statistical methods for model comparisons. In section 3, we evaluate the relationships between measured P, W, V, H, and A in MOPEX watersheds, and quantify the information about NDVI contained by each using orthogonal regressions. Results are first presented to identify the climate and catchment-landscape variables that control intercatchment variability in water balance described by the Horton index (sections 3.2 and 3.3), and second to independently evaluate the relationship between different climate variables and vegetation greenness (measured using NDVI), both with and without information on catchment water balance from the Horton index (section 3.4). Finally, we discuss implications for the development of catchment-hydrology models that use both climate and catchment landscape properties to predict the adaptive behavior of watersheds and their vegetation systems.

2. Methods

2.1. Data Collection and Processing

[9] A summary of all data and sources of data used in this study is contained in Table 1. We refer to precipitation, potential evapotranspiration, and the aridity index collectively as "climate" variables. Similarly, we refer to latitude, longitude, catchment area, mean catchment elevation, mean percent aspect, mean catchment slope, mean soil porosity, mean soil field capacity, mean soil wilting point, mean soil saturated conductivity, mean soil plant-available water, mean soil rock depth, and mean percent soil composition collectively as "landscape" characteristics.

2.1.1. Hydrometeorological Data

[10] We use a subset of the MOPEX data (Figure 2) [*Duan et al.*, 2006; *Schaake and Duan*, 2006] containing daily precipitation, minimum and maximum temperatures, discharge, and some physical characteristics for 431 U.S. catchments covering the period from 1948 to 2003. The drainage area of the selected catchments varies from the order of 10 to 10,000 km^2, covering a wide range of scales. Selected catchments span all major geological and climate regions in the United States, although there is a bias in selection toward the wetter, more populous, less-alpine, and more heavily monitored eastern United States. The data record for these catchments was expanded to cover the 2000–2008 water years (1 October 1999 through 30 September 2008) to obtain data contemporaneous with remote sensing indices of vegetation. Daily streamflow data were obtained from the U.S. Geological Survey (USGS) and precipitation and temperature data were obtained from the Oregon State University PRISM (Parameter-elevation Regressions on Independent Slopes Model) database [*Daly et al.*, 1994]. The monthly PRISM data at 4 km resolution were spatially averaged to create a time series of total precipitation and minimum and maximum temperatures for each catchment.

[11] Daily streamflow, Q, was partitioned into two components: base or slow flow, U, which represents the discharge from the groundwater storage to the stream, and direct runoff or quick flow, S, which is the response of the streamflow to rainfall and is affected by catchment characteristics. The one parameter recursive filter [*Lyne and Hollick*, 1979]

$$U_k = aU_{k-1} + \frac{1-a}{2}(Q_k + Q_{k-1}), \quad U_k \le Q_k, \tag{1}$$

where a is a filter parameter, was used to compute base flow and direct runoff ($S = Q - U$). The value of the filter parameter, a, was set to 0.925. This filter was passed over

Table 1. Summary of Study Catchment Data and Sources

	Source or Method[a]
Hydrometeorological Data	
Daily precipitation (mm)	MOPEX, PRISM
Daily min and max temperatures (°C)	MOPEX, PRISM
Daily streamflow (mm)	MOPEX, USGS
Daily surface runoff (mm) from streamflow	*Lyne and Hollick* [1979]
Daily base flow index	*Wolock* [2003]
Annual Horton index	*Troch et al.* [2009]
Monthly potential evapotranspiration (mm)	*Hamon* [1961]
Annual aridity index	*Troch et al.* [2009][b]
Landscape and Remote Sensing Data	
Normalized Difference Vegetation Index	NASA MODIS
Latitude, longitude, catchment area (km^2)	MOPEX
Mean catchment slope (percent)	SRTM
Mean elevation (m)	SRTM
Mean aspect (percent)	SRTM
Soil characteristics for 11 layers and depth to bedrock[c]	STATSGO
Vegetation type and land use classes	NLCD

[a]MOPEX, Model Parameter Estimation Experiment [*Duan et al.*, 2006]; PRISM, Parameter-elevation Regressions on Independent Slope Model [*Daly et al.*, 1994]; MODIS, Moderate Resolution Imaging Spectroradiometer [*Huete et al.*, 2002]; SRTM, Shuttle Radar Topography Mission [*Farr et al.*, 2007]; STATSGO, State Soil Geographic Database [*Miller and White*, 1998]; NLCD, National Land Cover Database [*Homer et al.*, 2004].

[b]*Troch et al.* [2009] use the humidity index, which is the reciprocal of aridity index.

[c]Soil characteristics include percent clay, percent silt, percent sand, mean soil porosity, mean soil field capacity, mean soil wilting point, mean so il saturated conductivity, mean soil plant available water, mean soil rock depth, and mean percent soil composition.

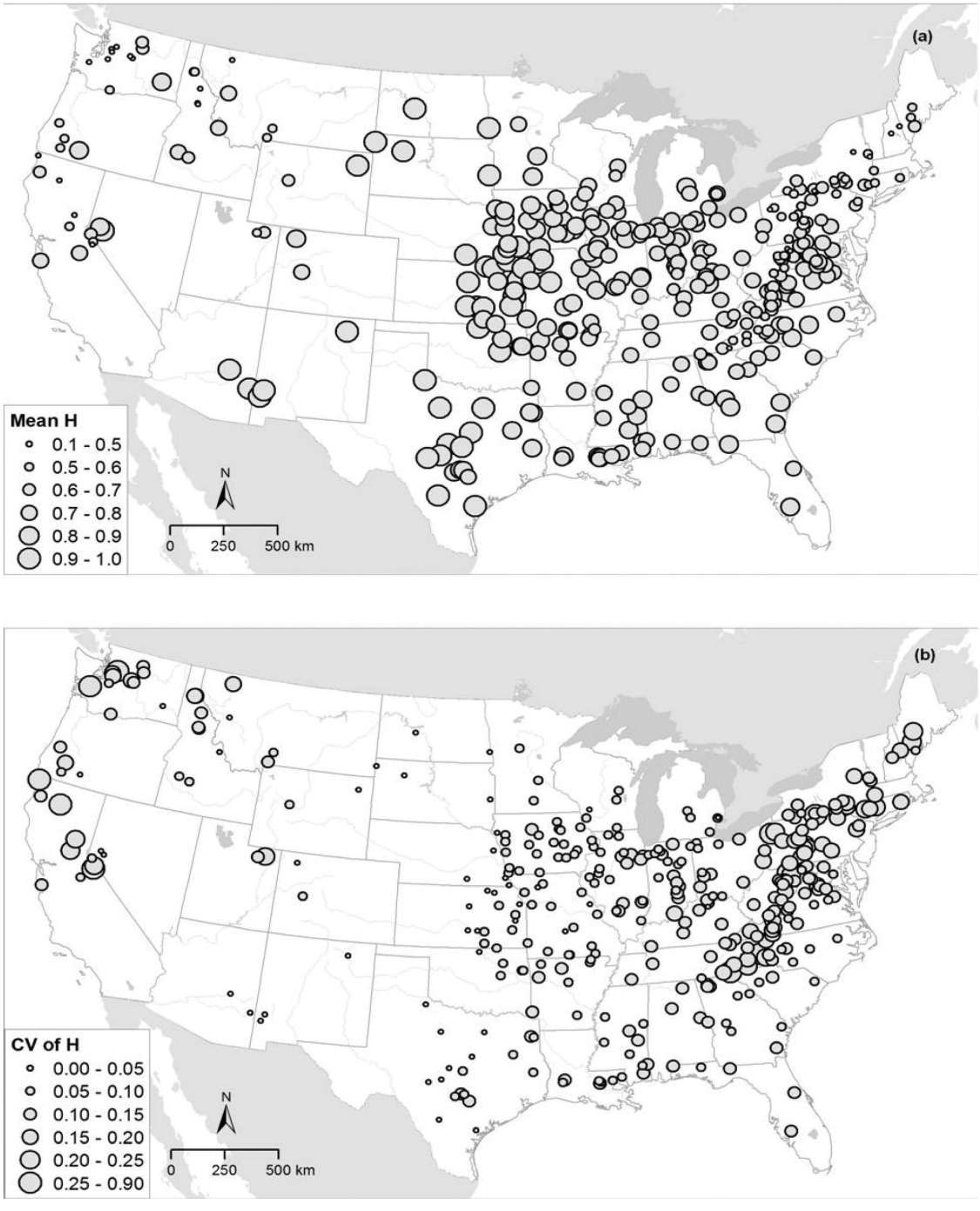

Figure 2. (a) Mean and (b) variability (coefficient of variation, CV) of the Horton index at the 361 MOPEX catchments used in this study.

the streamflow data twice, backward and forward in time, to obtain more precise estimation of the base flow especially for the beginning of the time series. *Troch et al.* [2009] concluded that estimates of the Horton index are not very sensitive to the type of base flow separation algorithm used.

[12] Daily values of streamflow, base flow, and direct runoff were summed to annual timescales. The annual values of streamflow (Q), base flow (U), and direct runoff (S) together with annual precipitation (P) data for each water year were used to estimate the vaporization-to-wetting ratio referred to as the Horton index (H) [*Troch et al.*, 2009]:

$$H = \frac{V}{W} = \frac{P - Q}{P - S}, \tag{2}$$

where wetting (W) is the portion of precipitation retained by the catchment at storm time scales and vaporization (V) is the portion of precipitation that does not eventually become streamflow via runoff or base flow. The average

Horton index was then derived using all relevant water years (e.g., 2000–2008 when comparing with the NDVI, see below). In addition, the average base flow index (U/Q) was computed for each catchment, as well as using the gridded base flow index data set developed by *Wolock* [2003] (Table 1). Monthly potential evapotranspiration (PET) was computed using Hamon's equation [*Hamon*, 1961] as formulated by *Wolock and McCabe* [1999]:

$$\mathrm{PET} = 13.97(d)(D)\rho_w, \qquad \rho_w = \frac{4.95e^{0.062T}}{100}, \tag{3}$$

where d is the number of days in a month, D is the mean monthly hours of daylight in units of 12 h, ρ_w is a saturated water vapor density, and T is the monthly mean temperature in °C, estimated from minimum and maximum temperatures as $(T_{\max} + T_{\min})/2$. Monthly hours of daylight were modeled using the algorithm described by *Forsythe et al.* [1995]. Annual values of potential evapotranspiration and precipitation were used to estimate the aridity index

$$A = \frac{\mathrm{PET}}{P}. \tag{4}$$

2.1.2. Remote Sensing Data

[13] The time series of NDVI for selected catchments were extracted from NASA's Moderate Resolution Imaging Spectroradiometer (MODIS) Land Products MOD13A2 distributed by the Land Processes Distributed Active Archive Center (LP DAAC), located at the USGS Earth Resources Observation and Science (EROS) Center (available at https://lpdaac.usgs.gov/). MOD13A2 stores NDVI composites every 16 d at the spatial resolution of 1 km [*Huete et al.*, 2002]. The remote sensing data quality is enforced using two quality filters. First, pixels with cloud cover were filtered from the data set. Second, because steeply sloped landscapes are known to yield MODIS data that are noisy and biased toward higher NDVI, the small number (<5.9% of any one catchment ecosystem) of montane pixels with slopes >40° were filtered from the data set to improve remote sensing data quality in keeping with standard practice [*Lau*, 1997; *Liu et al.*, 2009]. It is possible to correct for high slope and adjacency effects using radiative transfer models based on digital elevation models [*Richter*, 2009], but it is more defensible to simply drop contaminated pixels for this study. However, the conclusions of this paper highlight the role of the catchment slope in partitioning soil moisture and suggest that efforts to resolve NDVI in steep catchments may add value to future studies.

2.1.3. Catchment Topographic, Soil, and Land Use Characteristics

[14] The 3 arc-s (90 m) Shuttle Radar Topography Mission (SRTM) research grade data [*Farr et al.*, 2007] (available at http://www2.jpl.nasa.gov/srtm/srtmBibliography.html downloaded from http://dds.cr.usgs.gov/srtm/) were used to compute topographic characteristics (elevation, slope, aspect) using ArcGIS spatial analysis tools. The elevation, slope, and aspect data were spatially averaged for each catchment using zonal statistics and aspect data were tabulated to eight compass directions for each catchment.

[15] The multilayer soil characteristics data set based on the USDA State Soil Geographic Database (STATSGO) [*Miller and White*, 1998] was used to compute the percentage of soil texture class for 11 soil layers and the spatial average of the depth to bedrock. Soil data sets were downloaded from the soil information website at the Pennsylvania State University (available at http://www.soilinfo.psu.edu/).

[16] The percentage of vegetation type and land use classes within our catchments was estimated from 30 m from the National Land Cover Database (NLCD) 2001 [*Homer et al.*, 2004] using spatial statistical tools. NLCD data were obtained from the Multi-Resolution Land Characteristics (MRLC) Consortium website (available at http://www.mrlc.gov/about.php).

2.2. Statistical Methods

[17] Our first goal was to determine the climatic parameters that affect hydrological partitioning reflected in the mean Horton index (Figure 2a), and the mechanisms (wetting or vaporization) by which the effect propagates. We constructed scatterplots and correlation matrices for all potential climatic predictors of V, W, H, and the coefficient of variation of the Horton index (Figure 2b), CV(H). Plots were used to (1) quality control data and check for extreme outliers, (2) provide an initial summary of the relationship between all variables, (3) select potentially relevant variables for regression analyses, and (4) anticipate regression-variable transformations. We then developed a statistical model using both simple single-predictor and multiple linear regressions to relate climate variables to individual components of the water balance, the Horton index, and its coefficient of variation.

[18] If landscape characteristics play a significant role in determining the fraction of soil moisture used by vegetation then these characteristics should be correlated with residual error in the climate-Horton index models. Thus, we analyzed original and mean-normalized landscape characteristics to residuals of the climate-Horton index model, both climate-Horton index components (V, W) models, and the climate-coefficient of variation of the Horton index model. This analysis included scatterplot construction, variable transformation, and saturated stepwise regression, a computationally efficient procedure for selecting significant variables and interaction terms frequently used when there are a large number of potential predictor variables [*Chatterjee and Hadi*, 2006]. These analyses led to the development of a model that predicts the 8 year mean Horton index (its components and its coefficient of variation) of a catchment based on statistically significant climate and landscape variables. We chose to use mean-normalized climate and landscape characteristics so that all variates would be dimensionless and of similar scale.

[19] Finally, we compared the power of P, V, W, A, H and the climate-landscape predicted H to predict NDVI. To capture the sensitivity of NDVI to these parameters, we believe it is important to relate how the mean maximum annual NDVI relates to the means of each of these parameters in their extreme values. In the cases of P, W, H, and predicted H, there is a near-perpendicular asymptotic behavior of the slopes at the domain extremes: a shallow slope in how low H (high P or W) values relate to high NDVI values and an extremely steep slope in how high H (low P or W) values relate to low NDVI values (see Figures 5a, 5b, 5e,

and 5f). Standard regression methods, which minimize vertical error, assume error in the response with no error assumed in the predictor set. Since A and H are estimates that naturally have error associated with them, the use of standard regression methods to relate A or H to NDVI violates a fundamental regression assumption. To capture near-perpendicular asymptotes in some models while meeting regression requirements in all models, we must minimize both vertical and horizontal error in each model, which requires the use of orthogonal regression whereby model parameters are iterated to minimize model error. The drawback of using iteration to obtain model parameter estimates is that a theoretical distribution of model error does not exist; hence, we cannot evaluate models through parametric means (e.g., ANOVA or parameter t-test). Since our goal was to compare NDVI models, we must choose a common model structure that works well with each climate parameter considered, yet allows us a means to pairwise-evaluate climate-greenness models using nonparametric methods. The common model structure chosen to represent these relationships is of the form

$$\mathrm{NDVI} = a(1 - \exp[-c\{X - b\}])\ X > b, \tag{5a}$$

$$\mathrm{NDVI} = a(1 - \exp[-c\{b - X\}])\ 0 \le X < b, \tag{5b}$$

where a is the horizontal asymptote along the NDVI axis representing the maximum mean NDVI, b is the x-axis intercept, and c is the curvature. For monotonically increasing relationships between NDVI and the predictor variable, X, we use equation (5a); for monotonically decreasing relationships, we use equation (5b). Since it is not possible to directly obtain model parameter estimates by orthogonal regression of curves other than a straight line [*Draper*, 1992], we minimize vertical and horizontal error by independently iterating a, b, and c until the squared geometric error distance is minimized [*Ahn*, 2004]. We then pairwise-evaluate the models through use of a nonparametric measure of error and assume that the model with the smallest variance provides higher precision. Nonparametric methods do not require normality or homoscedasticity of model residuals. To confirm that the difference in model error variances is statistically significant at a 5% confidence level, we use the nonparametric squared-rank test for equal variances [*Conover*, 1999].

3. Results

3.1. Overview of Climate and Landscape Relationships in MOPEX Catchments

[20] Potential evapotranspiration is close to vaporization in humid catchments ($A < 1$), but exceeds vaporization in semiarid catchments ($A > 1$) because such watersheds are water-limited (Figure 3a). Surface runoff, S, is generally low in semiarid regions and precipitation and wetting are approximately equal (Figure 3b). In humid regions, however, a larger fraction of precipitation runs off and precipitation exceeds wetting. There is therefore a strong relationship between the aridity index and the Horton index (Figure 3c). In arid regions, where potential evapotranspiration is larger than vaporization and precipitation is approximately equal to wetting, we expect the aridity index to exceed the Horton index. In more humid regions, the difference between the aridity index and the Horton index becomes smaller.

[21] Isolating the effects of climate and landscape characteristics on H is not straightforward because of confounding interrelationships between these variables. For example, average temperature, and therefore PET tends to decrease with increasing elevation, and the steepest slopes are likewise found at the highest elevations. Therefore, a naive analysis using univariate statistical regressions reveals a deceptively strong inverse relationship between PET and slope, whereas a multivariate regression analysis can identify a third factor, temperature, as the primary control on PET. To assess the relative importance of landscape variables on hydrologic partitioning (section 3.3), we first must understand the combination of climate variables to which H is significantly sensitive (section 3.2). It is then possible in section 3.3 to understand the unique information about catchment-scale (local-scale) hydrologic partitioning added by landscape variable controls (i.e., H), above and beyond information provided by well-understood biome-scale (regional-scale) climate variable controls (i.e., A). Finally, in section 3.4, we present an empirical model predicting a catchment's mean peak greenness (NDVI) on the basis of the mean A and H, and investigate whether catchment-scale

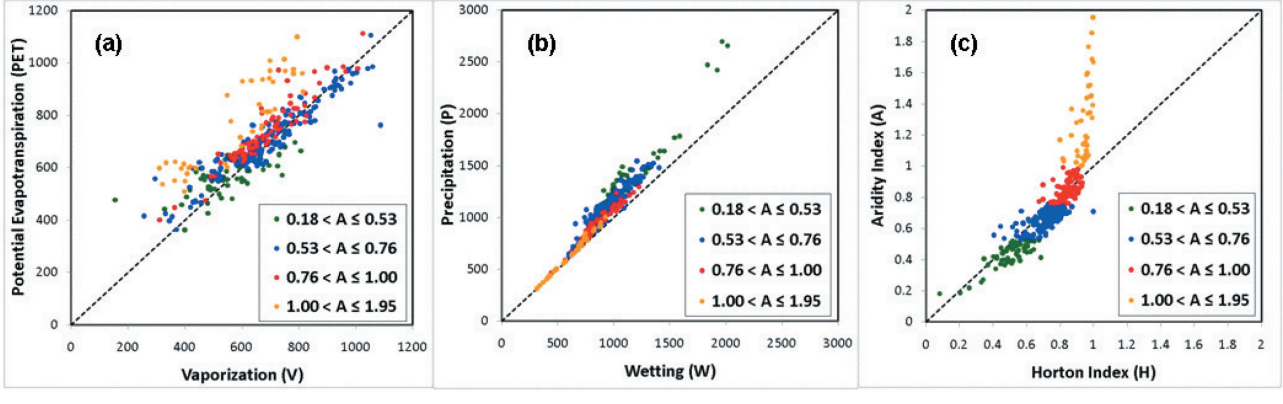

Figure 3. The relationship between (a) potential evaporation and estimated vaporization, (b) precipitation and soil wetting, and (c) Horton index and aridity index for the 361 MOPEX catchments shown in Figure 2.

vegetation indicates a significant response to the hydrologic partitioning processes controlled by landscape variables (i.e., H), in addition to regional-scale climate variables (i.e., A).

3.2. Influence of Regional-Scale Climate Variables on Hydrologic Partitioning

[22] Scatterplots and correlation analyses for the climate variables P and PET compared with Horton index components, V and W, the Horton index, H, and the coefficient of variation of the Horton index, CV(H), suggests power law relationships (i.e., a linear correlation between natural-logarithm-transformed variables) between climate variates and the Horton index variates. The multivariate combination of P and PET information has the most power in describing variations in V, H, and CV(H), while P has the most power in describing variations in W (Table 2). The combined power of ln P and ln PET increased explained variation in ln H by nearly 140% compared with a model including only the information in ln P.

[23] The resulting additive models for both ln H and ln CV(H) are

$$\ln \widehat{H} = -1.9 + 0.87 \ln \mathrm{PET} - 0.60 \ln P, \tag{6}$$

$$\ln \widehat{\mathrm{CV}(H)} = -5.7 - 1.6 \ln \mathrm{PET} + 2.0 \ln P, \tag{7}$$

where the circumflex symbol indicates the estimated value of the proposed model. Observe that regression slope coefficients in the H model as well as the CV(H) model are similar in magnitude but of opposite sign for ln P and ln PET (i.e., 0.87 and −0.60 are of similar magnitude in equation (6) and −1.6 and 2.0 have similar magnitude in equation (7)). Thus, we combine the P and PET into a single term and use a simpler model expressed as ln (PET/P), which is the natural logarithm of the aridity index, ln A:

$$\ln \widehat{H} = -0.10 + 0.65 \ln A, \tag{8}$$

$$\ln \widehat{\mathrm{CV}(H)} = -3.1 - 1.9 \ln A. \tag{9}$$

[24] The aridity-Horton index (A-H) model (equation (8)) explains slightly less variation in H ($R^2 = 0.75$ versus $R^2 = 0.80$) as compared with the additive model (equation (6)), but has higher statistical significance (Table 2) and results in a simpler and more dimensionally correct functional form. Similarly, the aridity-CV of Horton index (A-CV(H)) model (equation (9)) explains less variation ($R^2 = 0.60$ versus $R^2 = 0.62$) in CV(H) than the additive model (equation (7)), and has nearly double the statistical significance (Table 2).

[25] The aridity index A is therefore found to possess more predictive power for hydrologic partitioning (i.e., H), than any other tested combination of regional-scale climate variables. This finding is in line with conventional hydrologic understanding [*Budyko*, 1974; *Shuttleworth*, 1988], which holds that the first-order control on land-surface water balances and ecohydrology (i.e., vegetation productivity) is the relative scarcity of available water compared with available energy, as represented by the aridity index. The fitness of the A-H model is the highest when water and energy availability are roughly in balance, but this model based only on climate information is less powerful in the most arid and most humid regions where water-scarce or water-saturated conditions are present (Figure 4a). This result implies that additional second-order processes become more important for hydrologic partitioning in such regions. In section 3.3, we investigate whether catchment landscape properties can account for these observed deviations from the A-H model.

Table 2. Statistics for Climate-Horton Model Variable Selection

Response	Predictor	Estimate	t Ratio	F Ratio	R^2
ln V	Intercept	3.96	14.1	78.6	0.180
	ln P	0.36	8.87		
ln V	Intercept	−0.43	−1.75	787	0.687
	ln PET	1.05	28.05		
ln V	Intercept	−1.602	−6.59	565	0.759
	ln P	0.233	10.39		
	ln PET	0.987	29.36		
ln W	Intercept	0.906	13.47	7668	0.955
	ln P	0.851	87.56		
ln W	Intercept	4.47	10.33	28.6	0.074
	ln PET	0.356	5.37		
ln W	Intercept	0.261	2.66	4619	0.963
	ln P	0.836	92.33		
	ln PET	0.114	8.44		
ln H	Intercept	3.016	12.06	180	0.333
	ln P	−0.485	−13.42		
ln H	lntercept	−4.885	−13.56	160	0.308
	ln PET	0.697	12.63		
ln H	lntercept	−1.883	−8.49	693	0.795
	ln P	−0.597	−29.15		
	ln PET	0.870	28.35		
ln H	lntercept	−0.103	−10.47	1061	0.747
	ln A	0.654	32.58		
ln CV(H)	lntercept	−14.85	−20.67	299	0.455
	ln P	1.797	17.29		
ln CV(H)	Intercept	4.389	3.3	26.45	0.069
	ln PET	−1.047	−5.14		
ln CV(H)	Intercept	−5.70	−5.9	285	0.615
	ln P	2.00	22.49		
	ln PET	−1.62	−12.16		
ln CV(H)	Intercept	−3.100	−78.95	534	0.599
	ln A	−1.857	−23.11		

3.3. Influence of Catchment-Scale Landscape Variables on Hydrologic Partitioning

[26] Having developed models relating climate indices to the Horton index, H, its components, V and W, and its coefficient of variation, CV(H), we use the residuals of these models to identify landscape controls on partitioning. The correlation between the landscape variables and the residuals of the log linear climate-Horton models indicate significant second-order controls on hydrologic partitioning. Residuals for each of the best fit climate-Horton models ln H, ln V, ln W, and ln CV(H) will be denoted as $\widehat{e}(\ln H|\ln A)$, $\widehat{e}(\ln V|\ln P + \ln \mathrm{PET})$, $\widehat{e}(\ln W|\ln P + \ln \mathrm{PET})$, and $\widehat{e}(\ln CV(H)|\ln A)$, respectively. Of the 21 landscape characteristics we evaluated (Table 1), elevation (Z) and slope (β) have the strongest correlations with each of the four sets of residuals. Furthermore, untransformed elevation and slope had higher correlation with the residuals than their natural log transformations, ln Z and ln β, suggesting an exponential relationship between the landscape and the Horton index. The $\widehat{e}(\ln H|\ln A)$ residual set has moderate correlation values $|r| > 0.40$ with Z and β, and

the $\hat{e}(\ln V|\ln P + \ln \mathrm{PET})$, $\hat{e}(\ln W|\ln P + \ln \mathrm{PET})$, and $\hat{e}(\ln CV(H)|\ln A)$ residual sets have weak correlation values $|r| < 0.25$ with Z and β. This regression analysis confirms that the catchment landscape properties of elevation and slope, when added to the climate information contained in A, reduces the residual error encountered in extremely humid and extremely arid catchments when climate information alone is used to quantify catchment hydrologic partitioning (Table 3).

[27] The equation for the best-fit model, including catchment landscape information in addition to climate information, is

$$\ln \hat{H} = -0.085 + 0.53 \ln A + 0.036\beta + 0.13(\beta \times \ln A) - 0.061Z - 0.096(Z \times \ln A),$$

where $(\times)$ represents the interaction terms between $\ln A$ and the landscape variables. Exponentiating and rearranging yields a nonlinear form of the model,

Table 3. Statistics for Best-Fit Climate-Landscape-H Model

Predictor	Estimate	SE	t Ratio	p Value
Intercept	−0.0848	0.0116	−7.31	<0.0001
$\ln A$	0.532	0.0307	17.33	<0.0001
β	0.0362	0.0124	2.92	0.0037
Z	−0.0605	0.0107	−5.65	<0.0001
$\beta \times \ln A$	0.129	0.0109	11.83	<0.0001
$Z \times \ln A$	−0.0961	0.0163	−5.9	<0.0001

$$\hat{H} = \left(\frac{A^{0.53}}{e^{0.085}}\right)\left(\frac{A^{0.13}}{e^{-0.036}}\right)^{\beta}\left(\frac{A^{-0.096}}{e^{0.061}}\right)^{Z}. \quad (10)$$

[28] This empirically derived, nonlinear model for catchment hydrologic partitioning relates the 8 year (2000–2008) mean Horton index to aridity, slope, and elevation for 361 MOPEX catchments, and the functional form of this model suggests two significant observations. First, hydrologic partitioning as described by H is insensitive to the mean catchment slope at $A = \exp\{-0.036/0.13\} \approx 0.76$. In more

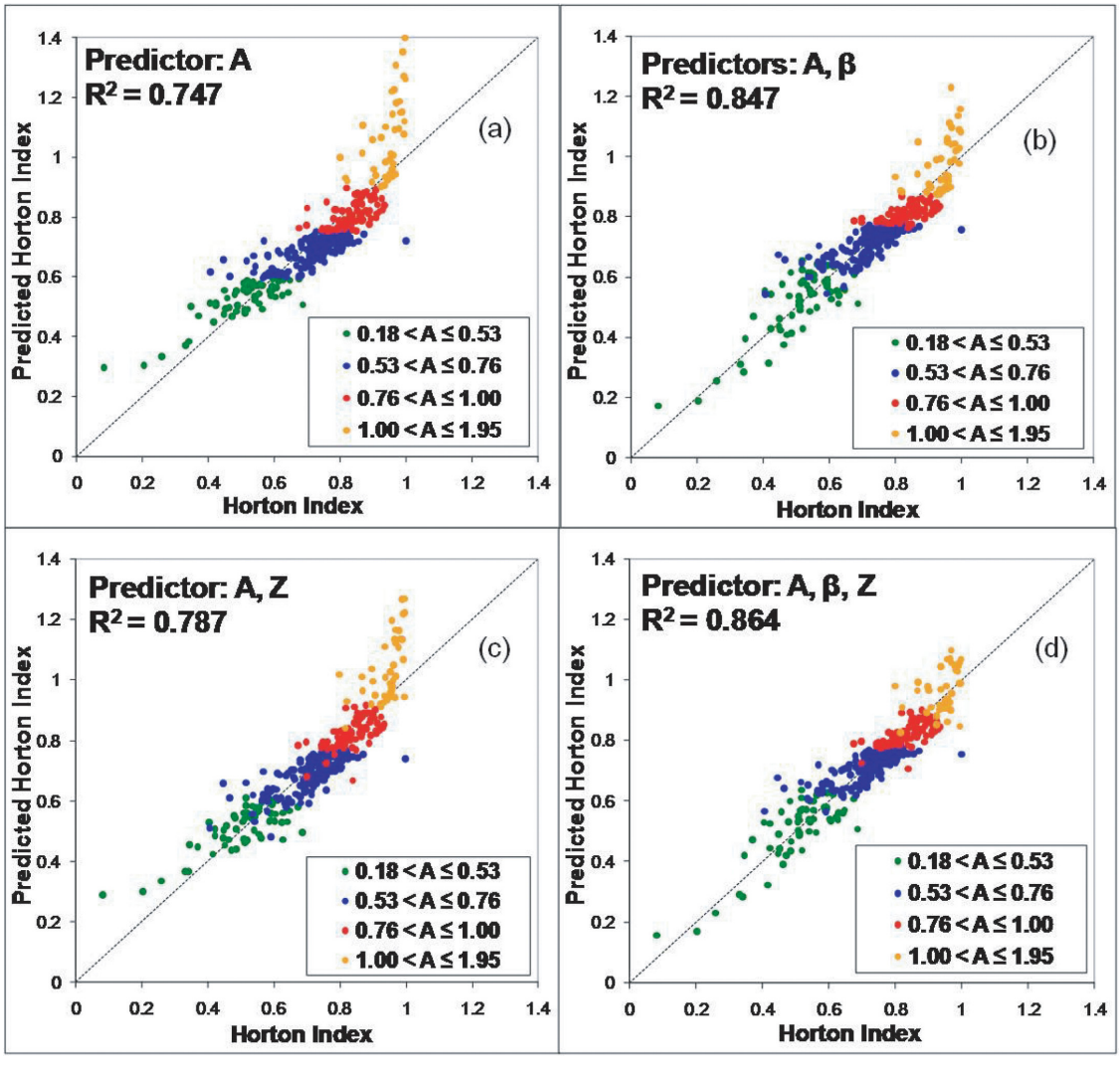

Figure 4. A comparison of the calculated and model predicted Horton index in 361 MOPEX catchments. While the fraction of soil moisture extracted by vegetation is largely a function of aridity index, A, slope (β), and elevation (Z), also affect H.

humid regions ($A < 0.76$), when slope increases, H decreases. In more arid regions ($A > 0.76$), when slope increases, H increases. Second, H is insensitive to elevation Z at $A = \exp\{-0.061/0.096\} \approx 0.53$. In more humid regions ($A < 0.53$), H increases with increasing catchment elevation. In more arid regions ($A > 0.53$), H decreases with increasing elevation. We will discuss these observations in section 4.

[29] The addition of elevation to the A-H model improved prediction of the Horton index significantly in arid regions (Figure 4c) and resulted in a 4% increase in model prediction overall (via R^2). Because there are relatively few sites in arid regions, this resulted in only a small increase in R^2. Inclusion of the mean catchment slope in the A-H model improved fit for all data (by 6.3%) and resulted in an increased model R^2 (Figure 4b). The combination of catchment mean slope (β) and elevation (Z) in addition to regional climate (A) describes 86% of the variation in the Horton index (Figure 4d), and tends to correct for H-prediction errors encountered when using only climate information to predict hydrologic partitioning in extremely humid and extremely arid catchments. Comparing the 86% explained by adding landscape variables against the 75% explained using only climate variables (an additional 11% explained variation in the Horton index by adding catchment landscape variables), it is possible to conclude that catchment landscape properties provide significant power to predict catchment hydrologic partitioning, in agreement with *Zhang et al.* [2008] and prior studies.

[30] Interestingly, while including Z and β as regression parameters improved the final model for H, the landscape parameters did not significantly improve the prediction for either the individual components of H (V, W) or CV(H). Elevation Z contributes only 0.21% and 0.14% of additional explained variation to V and W, respectively, whereas it contributes an additional 4.0% to H. Slope β contributes only 1.13% and 0.26% of additional explained variation to V and W, respectively, whereas it contributes an additional 10.0% to H. We thus conclude that neither V nor W is by itself strongly influenced by landscape characteristics because they are driven primarily by PET and P (see Figure 3). It is the ratio of V to W, and not the magnitude of the separate variables, that is more sensitive to catchment landscape properties.

[31] Recalling that H is the fraction of plant-available water that is partitioned into vaporization, these results indicate that catchment hydrologic partitioning (particularly water use by vegetation) is sensitive to the catchment landscape variables elevation and slope, and that this sensitivity increases for more arid and more humid catchments. The functional form in equation (10) describes three classes of catchments with respect to the effects of second-order landscape properties on hydrologic partitioning: class "A" ($A > 0.76$), class "B" ($0.53 < A < 0.76$), and class "C" ($A < 0.53$). In class A (more arid catchments), H is positively related to slope and negatively related to elevation. In class B (intermediate catchments), H is negatively related to both slope and elevation. In class C (more humid catchments), H is negatively related to slope and positively related to elevation. This result provides a new means of empirically classifying catchments into three typologies on the basis of hydrologic partitioning, and equation (10) provides a robust empirical function describing the control of regional-scale climate and catchment-scale landscape variables.

3.4. Added Information About Catchment Greenness Provided by Hydrologic Partitioning

[32] Now that we have established the significance of catchment landscape properties (slope and elevation) on catchment hydrologic partitioning, we will test the hypothesis that the Horton index (H) contains additional information about a catchment's vegetation system as compared to the aridity index (A). This hypothesis is reasonable given our results from sections 3.2 and 3.3, because H contains implicit information about the effects of catchment slope and elevation on plant-available water and vegetation water use (in addition to regional climate information). We will construct an orthogonally fitted empirical model predicting the catchment's 8 year average peak NDVI, based on landscape and climate variables. The corresponding null hypothesis holds that one of the tested catchment variables P, W, V, A, or H (see section 2 for details of variable computation) has equal or greater precision (measured as model error) to predict a catchment's vegetation patterns as measured by NDVI.

[33] To test our null hypothesis, we first evaluate the relationship between NDVI and P, W, V, A, and H at our study catchments, using the empirical function introduced in section 2 and labeled in Figure 5. There is a strong relationship between mean annual precipitation and NDVI (Figure 5a). However, the combination of P and PET in the form of $A = \mathrm{PET}/P$ has a much stronger relationship with NDVI than P alone (Figure 5d). To test the role of topographically induced partitioning of precipitation into plant-available water, we evaluated the relationship of NDVI with W, V, and H. The relationship between soil-wetting W and NDVI (Figure 5b) is similar to that of P and NDVI (Figure 5a). Surprisingly, there is no discernable relationship between vaporization V and NDVI (Figure 5c). The Horton index H, however, predicts NDVI with significantly less error than P, W, or V independently, and slightly lower error than A (the observed and model predicted relationships are presented in Figures 5e and 5f). Predictions of NDVI using H have a statistically significant advantage in error variance at the 5% confidence level using the nonparametric squared-rank test described in section 2. It is therefore possible to reject the null hypothesis that P, W, V, and A contain as much information about a catchment's vegetation as the Horton index (H), on the basis that a model predicting NDVI using the integration of climate and landscape information contained in H produces slightly better average prediction accuracy and a statistically significant improvement in error variance as compared with a model predicting NDVI using the best alternative, the aridity index, which contains only climate information. This result strengthens the findings in section 3.3 by establishing the importance of catchment-scale landscape properties as a modest but significant control on catchment hydrologic partitioning (as compared with the regional-scale climate properties contained in the aridity index), and by using remote sensing observations to confirm that vegetation responds to the modification of plant-available water by these catchment-scale landscape properties captured in the Horton index.

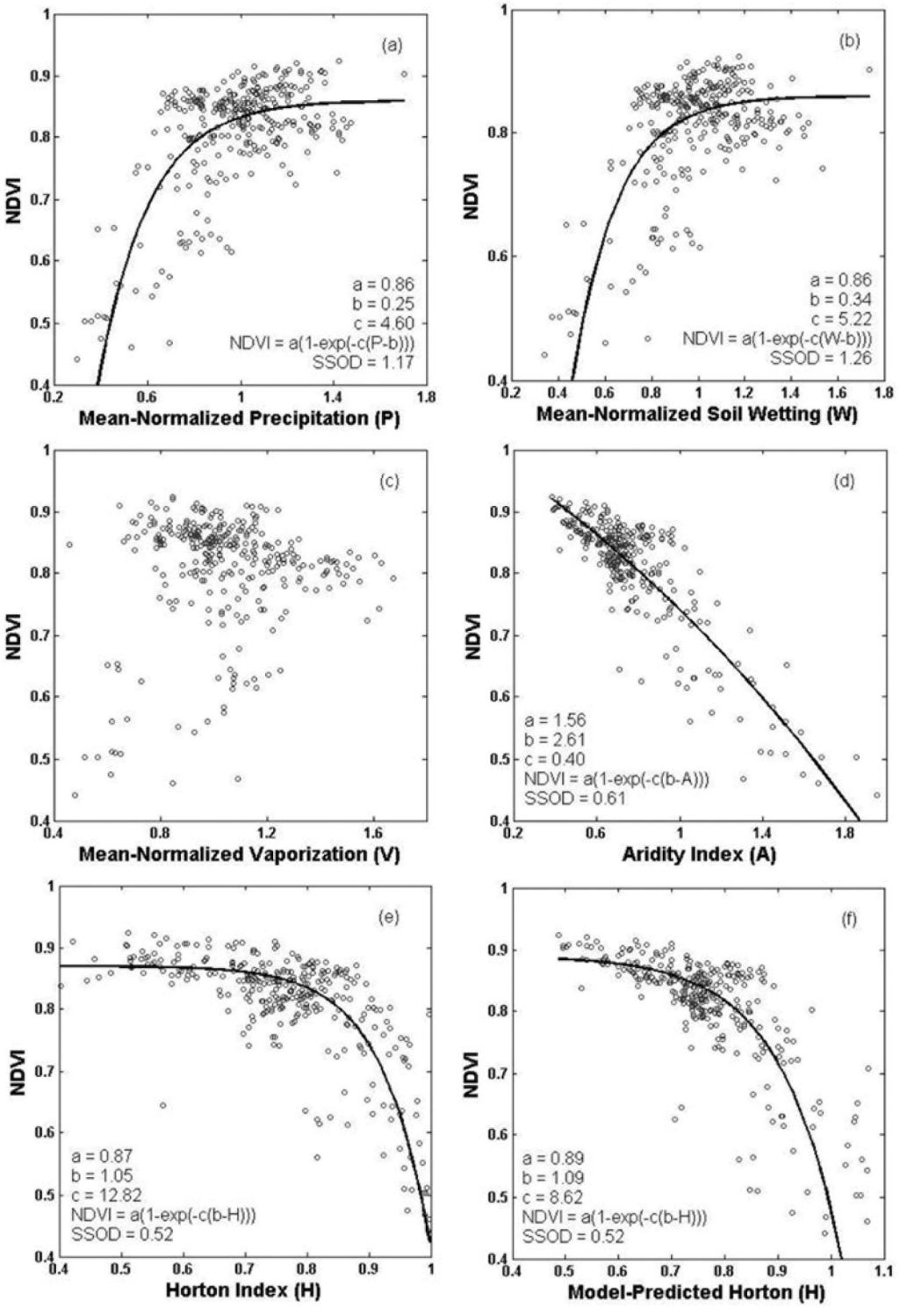

Figure 5. Scatterplots demonstrating the strength of the relationship between vegetation productivity and (a) precipitation, (b) soil-wetting, (c) vaporization, (d) aridity index, (e) measured Horton index, and (f) optional model-estimated Horton index from Figure 4d. Model error is measured using the sum of squared orthogonal distance (SSOD) from each data point to the regression line.

[34] The empirical models presented in Figure 5 apply only to catchments with a mean slope of <4%. When values of NDVI are plotted against P, W, V, A, and H for the 361 catchments selected for this study, a number of extreme outliers appear below the fitted model curves in Figure 5. These outliers represent a severe overprediction of NDVI using our statistical model, and 100% of these outlying catchments have a mean slope greater than ~4%. By filtering 361 catchments to remove from the sample all catchments with slope >4%, the resulting sample contains 312 catchments (87% of the original 361). The remaining 312 catchments span the same range of scales as the larger sample, between 80 and 10,328 km^2. The vast majority of the 49 removed catchments are in the Pacific Northwest and northern Rocky Mountains, where a combination of unique geology, alpine topography, snow and ice, slope aspect angle effects, extremely high elevations, and documented problems with MODIS remote sensing and PRISM precipitation data (due to slope and topography effects in alpine regions), create a complex combination of confounding factors both for the physics of catchment hydrology and the accuracy of the observational data. The model developed in section 3.4 is thus useful only for catchments with moderate-to-low average slopes. Although the model excludes catchments where landscape and topography effects on water balances are expected to be the most pronounced and interesting, it is important to note that this model finds significant effects of landscape and topography on water balance in catchments with the mildest and most typical terrain. Additional work to extend this model to high-slope catchments yields a more generalized model thereby increasing model power and usability.

4. Summary and Discussion

[35] This work solidifies and statistically quantifies previously proposed connections between climate, catchment-scale landscape properties, hydrologic partitioning, and vegetation response. First, we show that the Horton index (the ratio of plant water use to plant water availability at catchment scales) is a consistent and reproducible characteristic of specific catchments. Data from over 300 catchments across the conterminous United States indicates that the Horton index captures catchment hydrologic and ecologic responses across many scales, climates, and ecosystems. Such ecohydrologic coupling has been suggested for both the growing season [*Horton*, 1933; *Troch et al.*, 2009] and annual timescale [*Brooks et al.*, 2011]. The model parameters controlling the two-way competition of hydrologic partitioning (at the land surface and in the subsurface) exhibit clear spatial patterns between catchments, such that the catchments within the same climate region exhibit different partitioning properties depending on local landscape characteristics [*Brooks et al.*, 2011]. This modeling approach, especially the three classes of catchments defined on the basis of equation (10), may be instrumental to develop catchment classification frameworks, once the connection between these parameters and biophysical controls can be unraveled [*Sivapalan et al.*, 2011].

[36] Second, our analysis identifies empirically the different controls of hydrologic partitioning as quantified through the Horton index. Not surprisingly, the evidence shows a strong first-order control by the regional climate (quantified as the aridity index) but also reveals that the Horton index contains information about how climate interacts with landscape properties, more specifically with topography. Catchment slope and elevation leave clear fingerprints in the record of mean annual streamflow and suggest that the Horton index is the result of how climate variability is filtered through the landscape. Our work suggests that a readily available landscape characteristic (topography as opposed to, for instance, soil properties) exerts important control not only on hydrologic partitioning (well established in catchment hydrology) but also on ecosystem dynamics. While this concept may be obvious to landscape ecologists, topographic elements are not typically included in vegetation dynamics models. Slope and elevation add a modest but significant predictive skill, when combined with climate information, to understand how water is partitioned at the catchment scale within climate regions, and this information propagates to control how vegetation ecosystems respond to climate variability [*Brooks et al.*, 2011] and climate gradients.

[37] Slope appears to be the dominant catchment landscape property control, most plausibly because it affects the competition between vaporization (V) and base flow (U). In other words, infiltrated precipitation (W) is more likely to contribute to base flow in steeper catchments, presumably because its residence time is shorter and thus available to vegetation use (V) for a shorter period than in less steep catchments [*Bertoldi et al.*, 2006; *McGuire*, 2008; *Reggiani et al.*, 2000; *Yokoo et al.*, 2008]. However, the role of slope is different in arid versus humid catchments. In arid catchments, increasing slope leads to an increasing Horton index, thus higher vegetation water use efficiency. This may be due to lateral subsidy along flow paths that result in spatial vegetation patterns along channel networks [e.g., *Rango et al.*, 2005]. Because slope appears to be very important even in low and moderate slope catchments, more work is needed to investigate the combined effects of slope and elevation on hydrological partitioning, particularly in very humid and very arid climates. Even after the effects of elevation on climate (T, PET) are taken into account, elevation still appears to play a role in the partitioning of W and is likely responsible for the way catchments store water. More work is needed to explore whether the observed elevation effects are related to vegetation type (woody versus herbaceous), soil properties (depth, porosity), fraction of water as ice/snow, some other catchment property, or an unknown observational error.

[38] Finally, the relationship between the Horton index, climate, and topography suggests links with vegetation dynamics. Vaporization (V) as mediated by vegetation within water and energy availability constraints is typically the largest component of a catchment water balance. Wetting (W) imposes upper bounds of water availability at the catchment scale, and slope controls the timescales that define the competition between V and W. Our statistical analysis shows that the Horton index (V/W) estimated from the catchment water balance or predicted from climate and topography is the best predictor (compared to annual precipitation P, potential evapotranspiration PET or their ratio, the aridity index A) of catchment greenness quantified by means of the maximum annual normalized difference vegetation index (NDVI). Notwithstanding that aridity is clearly related to vegetation productivity [*Huxman et al.*, 2004],

the Horton index explains more variability, especially in very humid and in very arid climate regions (recall the results in sections 3.2 and 3.3), because it relates to how catchments store and retain water that is available for vegetation. Since the aridity index and Horton index are estimates having error associated with them, relating each to NDVI required orthogonal fitting, which minimizes both vertical and horizontal error. The differential behavior of three classes of catchments derived on the basis of equation (10) suggests that catchment slope and elevation play different roles in humid versus arid climates and raises interesting questions about physical controls on water balance partitioning and vegetation dynamics.

[39] Our results highlight the role of the interaction between climate and the landscape in controlling water balance and vegetation response. We speculate that this new insight of how hydrologic and ecologic dynamics interact across different climates and landscapes can help us to predict how terrestrial ecosystems may respond to climate change. Our results indicate that it is not climate by itself, but climate interaction with the landscape that controls ecosystems response to climate change. The fact that the Horton index is surprisingly constant from year to year (Figure 2b), despite significant variations in annual precipitation [*Troch et al.*, 2009], points toward ecosystem resilience resulting from adaptation, acclimation, and assemblage strategies under current climate conditions and facilitated by landscape properties. Possible trajectories of ecosystem development during rapid climate change episodes will be conditioned by how future climate interacts with the landscape and thus how the ecohydrological system will coevolve.

[40] **Acknowledgments.** Work on this paper commenced during the Summer Institute organized at the University of British Columbia (UBC) during June–July 2009 as part of the NSF-funded project: Water Cycle Dynamic in a Changing Environment: Advancing Hydrologic Science through Synthesis (NSF grant EAR-0636043, M. Sivapalan, PI). We acknowledge the support and advice of numerous participants at the Summer Institute (students and faculty mentors). Thanks also due to Marwan Hassan and the Department of Geography of UBC for hosting the Summer Institute and for providing outstanding facilities, without this work would not have been possible. We would also like to thank the reviewers and Associate Editor for their constructive comments, which greatly improved this manuscript. R.S. was partially supported by NSF grant EAR-0817073.

References

Ahn, S. J. (2004), *Least Squares Orthogonal Distance Fitting of Curves and Surfaces in Space*, 125 pp., Springer, Berlin, Germany.

Bertoldi, G., R. Rigon, and T. M. Over (2006), Impact of watershed geomorphic characteristics on the energy and water budgets, *J. Hydrometeorol.*, *7*(3), 389–403.

Brooks, P. D., P. A. Troch, M. Durcik, E. L. Gallo, B. G. Moravec, M. E. Schlegel, and M. Carlson (2011), Quantifying regional-scale ecosystem response to changes in precipitation: Not all rain is created equal, *Water Resour. Res.*, *47*, W00J08, doi:10.1029/2010WR009762.

Brutsaert, W. (1988), The parameterization of regional evaporation—some directions and strategies, *J. Hydrol.*, *102*(1–4), 409–426.

Budyko, M. I. (1974), *Climate and Life*, 508 pp., Elsevier, New York.

Chatterjee, S., and A. S. Hadi (2006), *Regression Analysis By Example*, 4th ed., 375 pp., John Wiley, Hoboken, N. J.

Choudhury, B. J. (1994), Synergism of multispectral satellite-observations for estimating regional land-surface evaporation, *Remote Sens. Environ.*, *49*(3), 264–274.

Conover, W. J. (1999), *Practical Nonparametric Statistics*, 3rd ed., 584 pp., John Wiley, New York.

Daly, C., R. P. Neilson, and D. L. Phillips (1994), A statistical-topographic model for mapping climatological precipitation over mountanious terrain, *J. Appl. Meteor.*, *33*, 140–158.

Donohue, R. J., M. L. Roderick, and T. R. McVicar (2007), On the importance of including vegetation dynamics in Budyko's hydrological model, *Hydrol. Earth Syst. Sci.*, *11*(2), 983–995.

Draper, N. R. (1992), Straight line regression when both variables are subject to error., paper presented at Proceedings of the 1991 Kansas State University Conference on Applied Statistics in Agriculture.

Duan, Q., J. Schaake, V. Andre Assian, S. Franks, and G. Goteti (2006), Model Parameter Estimation Experiment (MOPEX): An overview of science strategy and major results from the second and third workshops, *J. Hydrol.*, *320*(1–2), 3–17.

Eagleson, P. S. (1978), Climate, soil, and vegetation 4. The expected value of annual evapotranspiration, *Water Resour. Res.*, *14*, 731–739, doi:10.1029/WR014i005p00731.

Farr, T. G., et al. (2007), The shuttle radar topography mission, *Rev. Geophys.*, *45*, RG2004, doi:10.1029/2005RG000183.

Fisher, J. B., K. Tu, and D. D. Baldocchi (2008), Global estimates of the land-atmosphere water flux based on monthly AVHRR and ISLSCP-II data, validated at 16 FLUXNET sites, *Remote Sens. Environ.*, *112*(3), 901–919.

Forsythe, W. C., R. S. Stahl, H. Wu, and R. M. Schoolfield (1995), A model comparison for daylength as a function of latitude and day of year, *Ecol. Modell.*, *80*(1), 87–95.

Frouin, R., and R. T. Pinker (1995), Estimating photosynthetically active radiation (PAR) at the Earth's surface from satellite-observations, *Remote Sens. Environ.*, *51*(1), 98–107.

Gerrits, A. M. J., H. H. G. Savenije, E. J. M. Veling, and L. Pfister (2009), Analytical derivation of the Budyko curve based on rainfall characteristics and a simple evaporation model, *Water Resour. Res.*, *45*, W04403, doi:10.1029/2008WR007308.

Goetz, S. J., and S. D. Prince (1999), Modelling terrestrial carbon exchange and storage: Evidence and implications of functional convergence in light-use efficiency, *Adv. Ecol. Res.*, *28*, 57–92.

Hamon, W. R. (1961), Estimating potential evapotranspiration, *J. Hydraul. Div. Proc. Am. Soc. Civil Eng.*, *87*, 107–120.

Hanan, N. P., S. D. Prince, and A. Begue (1995), Estimation of absorbed photosynthetically active ratiation and vegetation net production efficiency using satellite data, *Agric. Forest Meteorol.*, *76*(3–4), 259–276.

Hatton, T. J., G. D. Salvucci, and H. I. Wu (1997), Eagleson's optimality theory of an ecohydrological equilibrium: Quo vadis?, *Functional Ecology*, *11*(6), 665–674.

Homer, C., C. C. Huang, L. Yang, B. Wylie, and M. Coan (2004), Development of a 2001 National Landcover Database for the United States, *Photogramm. Eng. Remote Sens.*, *70*(7), 829–840.

Horton, R. E. (1933), The role of infiltration in the hydrologic cycle, *Trans. Amer. Geophys. Union*, *14*, 446–460.

Huete, A., K. Didan, T. Miura, E. P. Rodriguez, X. Gao, and L. G. Ferriera (2002), Overview of the radiometric and biophysical performance of the MODIS vegetation indices, *Remote Sens. Environ.*, *83*(1–2), 195–213.

Hutjes, R. W. A., et al. (1998), Preface: Biospheric aspects of the hydrological cycle, *J. Hydrol.*, *213*(1–4), 1–21.

Huxman, T. E., M. D. Smith, P. A. Fay, A. K. Knapp, M. R. Shaw, M. E. Loik, S. D. Smith, D. T. Tissue, J. C. Zak, J. F. Weltzin, et al. (2004), Convergence across biomes to a common rain-use efficiency, *Nature*, *429*(6992), 651–654.

Lau, C.-C. (1997), Geomorphologic Distribution of Normalized Difference Vegetation Index, paper presented at Asian Association of Remote Sensing, Kuala Lumpur, Malaysia.

Liu, Y., Y. Yamaguchi, and C. Ke (2009), Discrepancy between ASTER- and MODIS-derived land surface temperatures: Terrain effects, *Sensors*, *9*(2), 1054–1066.

L'vovich, M. I. (1979), *World Water Resources and Their Future*, 415 pp., Amer. Geophys. Union, Washington D. C.

Lyne, V., and M. Hollick (1979), Stochastic time-variable rainfall-runoff modelling, paper presented at Hydrology and Water Resources Symposium, Institution of Engineers Australia, Perth.

McGuire, J. J. (2008), Seismic cycles and earthquake predictability on east pacific rise, *Seismological Soc. Am.*, (3), 1067–1084.

Miller, D. A., and R. A. White (1998), A conterminous United States multilayer soil characteristics data set for regional climate and hydrology modeling, *Earth Interactions*, *2*(2), 1–26, doi:10.1175/1087-3562(1998)002<0002:CUSMS>2.0.CO;2.

Milly, P. C. D., R. T. Wetherald, K. A. Dunne, T. L. Delworth (2008), Climate change—Stationarity is dead: Whither water management?, *Science*, *319*(5863), 573–574.

Ponce, V. M., and A. V. Shetty (1995), A conceptual-model of catchment water-balance. 1. Formulation and calibration, *J. Hydrol.*, *173*(1–4), 27–40.

Porporato, A., E. Daly, and I. Rodriguez-Iturbe (2004), Soil water balance and ecosystem response to climate change, *American Naturalist*, *164*(5), 625–632.

Rango, A., L. Huenneke, M. Buonopane, J. E. Herrick, and K. M. Havstad (2005), Using historic data to assess effectiveness of shrub removal in southern New Mexico, *J. Arid Environ.*, *62*(1), 75–91.

Reggiani, P., M. Sivapalan, and S. M. Hassanizadeh (2000), Conservation equations governing hillslope responses: Exploring the physical basis of water balance, *Water Resour. Res.*, *36*(7), 1845–1863.

Richter, R. (2009), Atmospheric/Topographic Correction for Satellite Imagery, in ATCOR-2/3 User Guide, 152 pp., DLR, German Aerospace Center, Wessling, Germany.

Schaake, J., and Q. Y. Duan (2006), Preface: The model parameter estimation experiment (MOPEX), *J. Hydrol.*, *320*(1–2), 1–2.

Schymanski, S. J. (2008), Optimality as a concept to understand and model vegetation at different scales, *Geography Compass*, *2*(5), 1580–1598.

Schymanski, S. J., M. L. Roderick, M. Sivapalan, L. B. Hutley, and J. Beringer (2007), A test of the optimality approach to modelling canopy properties and CO2 uptake by natural vegetation, *Plant, Cell Environ.*, *30*, 1586–1598.

Shuttleworth, W. J. (1988), Macrohydrology—the new challenge for process hydrology, *J. Hydrol.*, *100*(1–3), 31–56.

Sivapalan, M., M. A. Yaeger, C. J. Harman, X. Xu, and P. A. Troch (2011), Functional model of water balance variability at the catchment scale. 1: Evidence of hydrologic similarity and space-time symmetry, *Water Resour. Res.*, *47*, W02522, doi:10.1029/2010WR009568.

Szilagyi, J., D. C. Rundquist, D. C. Gosselin, and M. B. Parlange (1998), NDVI relationship to monthly evaporation, *Geophys. Res. Lett.*, *25*(10), 1753–1756, doi:10.1029/98GL01176.

Thompson, S. E., C. J. Harman, A. G. Konings, M. Sivapalan, A. Neal, and P. A. Troch (2011a), Comparative hydrology across AmeriFlux sites: The variable roles of climate, vegetation, and groundwater, *Water Resour. Res.*, *47*, W00J07, doi:10.1029/2010WR009797.

Thompson, S. E., C. J. Harman, P. A. Troch, P. D. Brooks, and M. Sivapalan (2011b), Spatial scale dependence of ecohydrologically mediated water balance partitioning: A synthesis framework for catchment ecohydrology, *Water Resour. Res.*, *47*, W00J03, doi:10.1029/2010WR009998.

Troch, P. A., G. F. Martinez, V. R. N. Pauwels, M. Durcik, M. Sivapalan, C. Harman, P. D. Brooks, H. Gupta, and T. Huxman (2009), Climate and vegetation water use efficiency at catchment scales, *Hydrol. Process.*, *23*(16), 2409–2414.

Wagener, T. (2007), Can we model the hydrological impacts of environmental change?, *Hydrol. Process.*, *21*(23), 3233–3236.

Wolock, D. M. (2003), Base-flow index grid for the conterminous United States, in *U.S. Geological Survey Open-File Report 03-263*, Reston, VA.

Wolock, D. M., and G. J. McCabe (1999), Explaining spatial variability in mean annual runoff in the conterminous United States, *Clim. Res.*, *11*(2), 149–159.

Yang, D. W., D, W. Shao, P. J.-F. Yeh, H. Yang, S. Kanae, and T. Oki (2009), Impact of vegetation coverage on regional water balance in the nonhumid regions of China, *Water Resour. Res.*, *45*, W00A14, doi:10.1029/2008WR006948.

Yokoo, Y., M. Sivapalan, and T. Oki (2008), Investigating the roles of climate seasonality and landscape characteristics on mean annual and monthly water balances, *J. Hydrol.*, *357*(3–4), 255–269.

Zhang, L., N. Potter, K. Hickel, Y. Zhang, and Q. Shao (2008), Water balance modeling over variable time scales based on the Budyko framework—Model development and testing, *J. Hydrol. 360*(1–4), 117–131.

P. D. Brooks, M. Durcik, A. Neal, and P. A. Troch, Department of Hydrology and Water Resources, University of Arizona, 1133 E. James E. Rogers Way, Tucson, AZ 85721, USA.

B. Ruddell, Department of Engineering, Arizona State University—Polytechnic, 7231 E. Sonoran Arroyo Mall, Mesa, AZ 85212, USA.

R. Schumer and H. Voepel, Division of Hydrological Sciences, Desert Research Institute, 2215 Raggio Pkwy., Reno, NV 89512, USA. (rina@dri.edu)

M. Sivapalan, Department of Civil and Environmental Engineering, University of Illinois at Urbana-Champaign, 205 N. Matthews Ave., Urbana, IL 61801, USA.